varian

FED L

ORNL/Sub-~~79~~ 80/21453/ 5

cy. 24

60 GHz GYROTRON DEVELOPMENT PROGRAM

J.F. Shively, T.J. Grant, A.L. Nordquist,
D.S. Stone, and G.E. Wendell

Quarterly Report No. 5

July through September 1980

FUSION ENERGY DIVISION LIBRARY

Prepared for:

OAK RIDGE NATIONAL LABORATORY

OAK RIDGE, TENNESSEE 37830

Operated by:

UNION CARBIDE CORPORATION

FOR THE DEPARTMENT OF ENERGY

CONTRACT NO. W-7405-ENG-26

Varian Associates, Inc.
Palo Alto Microwave Tube Division
611 Hansen Way
Palo Alto, California 94303

ORNL/Sub-79/21453/5

60 GHz GYROTRON DEVELOPMENT PROGRAM

J. F. Shively, T. J. Grant, A. L. Nordquist, D. S. Stone
and G. E. Wendell

Quarterly Report No. 5

July through September 1980

Prepared for:
Oak Ridge National Laboratory
Oak Ridge, Tennessee 37830

Operated by:
Union Carbide Corporation
for the
Department of Energy
Contract No. W-7405-eng-26

Varian Associates, Inc.
Palo Alto Microwave Tube Division
611 Hansen Way
Palo Alto, California 94303

P. O. 53Y-21453C

TABLE OF CONTENTS

Section		Page No.
I.	INTRODUCTION	1
II.	ELECTRON GUN	2
III.	SUPERCONDUCTING SOLENOID MAGNET	7
IV.	OUTPUT/COLLECTOR	9
	A. Mode Conversion at Conical Taper to Cylindrical Junctions	9
	B. Electron Trajectory Calculations	22
V.	WINDOW	24
VI.	COMPONENTS	25
	A. Waterloads	25
	B. Frequency Sampler and Arc Detector	25
	C. Mode Filters	25
VII.	TUBE ASSEMBLY	27
	A. VGE-8060 S/N X-1 (First Experimental Pulsed Tube)	27
	B. VGE-8060 S/N 1 (First 100 ms Pulse Duration Tube)	27
	C. VGE-8060 S/N 2 (Second 100 ms Pulse Duration Tube)	28
VIII.	PROGRAM SCHEDULE AND PLANS	29
IX.	REFERENCES	35

LIST OF ILLUSTRATIONS

Figure		Page No.
1.	Gradients for Original Gun Pulsed On	3
2.	Magnified View of Gradients for the Original Gun ...	4
3.	Gradients for Modified Gun	6
4.	Variation of the Mode Conversion Parameter, T_{m1}, with the Transductance Parameter K	10
5.	Variation of the Mode Conversion Parameter, T_{m2}, with the Transductance Parameter K	11
6.	Variation of the Mode Conversion Parameter, T_{m3}, with the Transductance Parameter K	12
7.	Variation of the Mode Conversion Parameter, T_{m4}, with the Transductance Parameter K	13
8.	Variation of the Mode Conversion Parameter, T_{m5}, with the Transductance Parameter K	14
9.	Variation of the Mode Conversion Parameter, T_{66}, with the Transductance Parameter K	15
10.	Mode Conversion, P_{m1}	16
11.	Mode Conversion, P_{m2}	17
12.	Mode Conversion, P_{m3}	18
13.	Mode Conversion, P_{m4}	19
14.	Mode Conversion, P_{m5}	20
15.	Mode Conversion, P_{m6}	21
16.	Milestone Chart and Status Report	30

LIST OF TABLES

Table		Page No.
I.	Voltage Gradients	5
II.	Superconducting Solenoid Magnet Dewar Cryogenic Data	8
III.	Collector Trajectory Landing Sites	23

ABSTRACT

The objective of this program is to develop a microwave oscillator capable of producing 200 kW of CW output power at 60 GHz. The use of cyclotron resonance interaction is being pursued.

The design, procurement and early construction phases of this program are discussed.

I. INTRODUCTION

The objective of this program is to develop a microwave oscillator designed to produce 200 kW of CW output power at 60 GHz. Neither tunability nor bandwidth are considered important parameters in the design but efficiency is. Mode purity in the output waveguide is not a requirement for the device, but the circular electric mode is considered desirable because of its low loss properties.

With these objectives in mind, an approach based on cyclotron resonance interaction between an electron beam and microwave fields is being pursued. The detailed arguments leading to this approach are contained in the final report of a preceding study program[1]. The device configurations of particular interest, called gyrotrons, have been discussed in recent literature[2-6]. They employ a hollow electron beam interacting with cylindrical resonators of the TE_{0M1} class.

The optimum beam for the cyclotron resonance interaction is one in which the electrons have most of their energy in velocities perpendicular to the axial magnetic field. Another requirement is that the spread in the axial components of the electron velocities be as small as possible. Electrons which have different axial velocities will not interact efficiently.

The approach chosen to generate the beam is a magnetron type of gun as is used on the 28 GHz gyrotron, also developed for Oak Ridge National Laboratory[7,8]. With this type of gun the shaping of the magnetic field in the gun region becomes quite important.

Construction of the experimental pulsed 60 GHz gyrotron is continuing. Electron gun parts have been received and construction will begin next quarter. A successful superconducting solenoid magnet design review was held at Magnetic Corporation of America. Coil winding has begun. Collector construction is nearly complete. Nearly all of the window parts have been received and a braze jig for the window is being machined. At present, the limiting item appears to be modification of the test set.

II. ELECTRON GUN

The 60 GHz gun design was subjected to computer analysis this quarter for the purpose of calculating the magnitudes of the DC electric field normal to the surfaces of the negatively-biased electrodes. This work was done to ensure that surface gradients would contribute minimally to the generation of an arc in the gun region.

The calculations were done using a Varian computer program which solves Laplace's equation in cylindrical coordinates (by finite element methods) for the potential in a given two-dimensional region. The fields were then determined by calculating the gradient of the potential distribution in a desired direction. Surface gradients were then obtained by matching a power dependence on radius of the field to calculated values near the electrode, and extrapolating to the electrode surface.

Figure 1 depicts a computer-generated plot of the electrical geometry in the gun region, showing the cathode support and focusing structure, the gun anode, and the body of the tube. It also includes the presence of the gun ceramic and the solenoid dewar. The gun ceramic is modeled as a finite thickness cylinder in the computer program. The figure shows the potential distribution when the tube is turned on (i.e., with the gun anode at 25 kV and the body at 80 kV with respect to the cathode potential). The surface gradient was calculated both for this configuration (turned-on) and the turned-off case, with the gun anode biased 2 kV below cathode. In general, the surface gradient was higher for the turned-off case at the gun anode surface, and was higher in the turned-on case at the tip of the cathode structure (front focus electrode).

Attention was focused on finding the location of the maximum surface gradients of the gun anode and cathode front focus electrode. These two areas are shown in Figure 1. Figure 2 is a magnified view of these two locations, indicating where the surface gradient was calculated to be maximum.

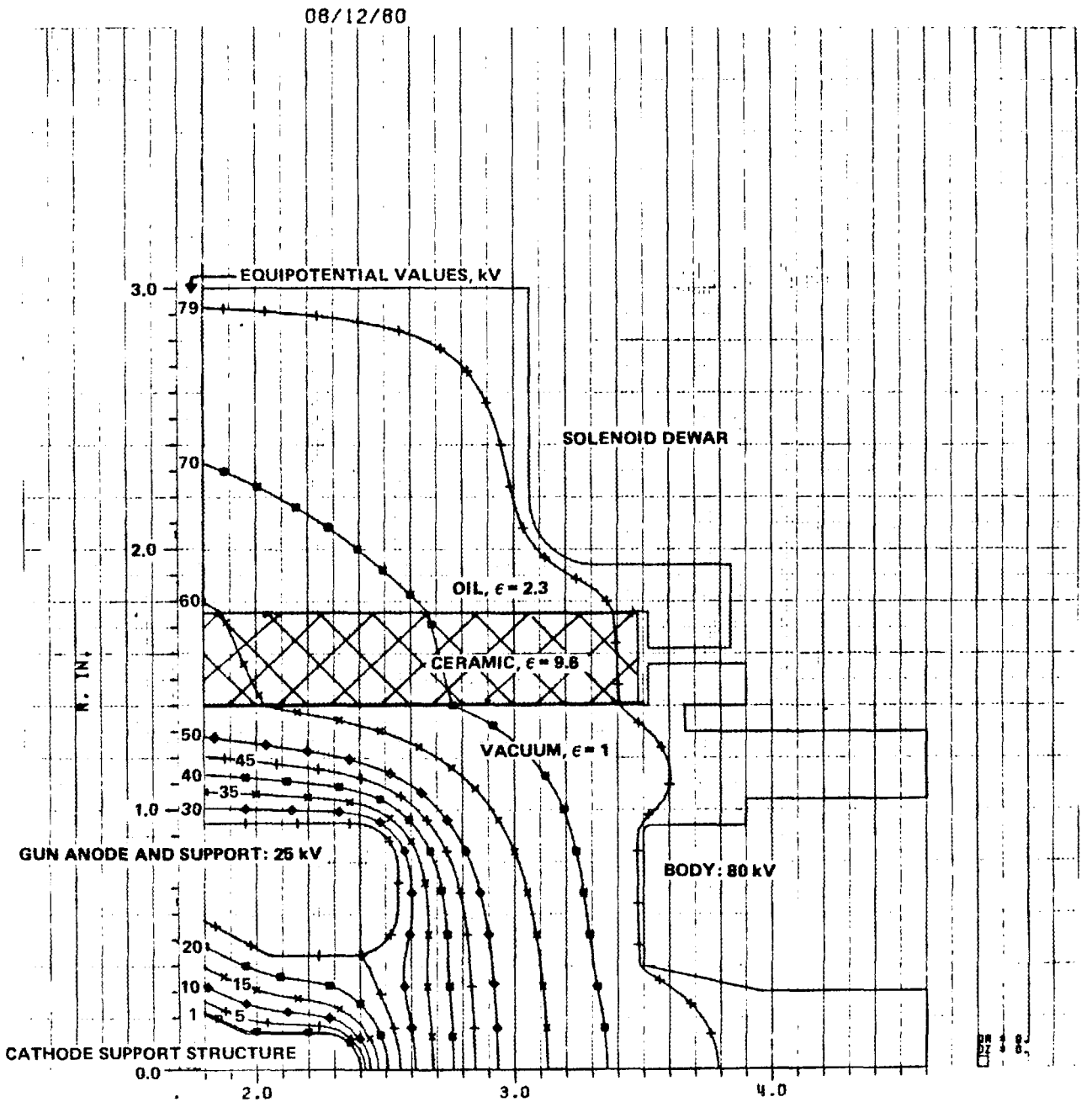

FIGURE 1: GRADIENTS FOR ORIGINAL GUN PULSED ON

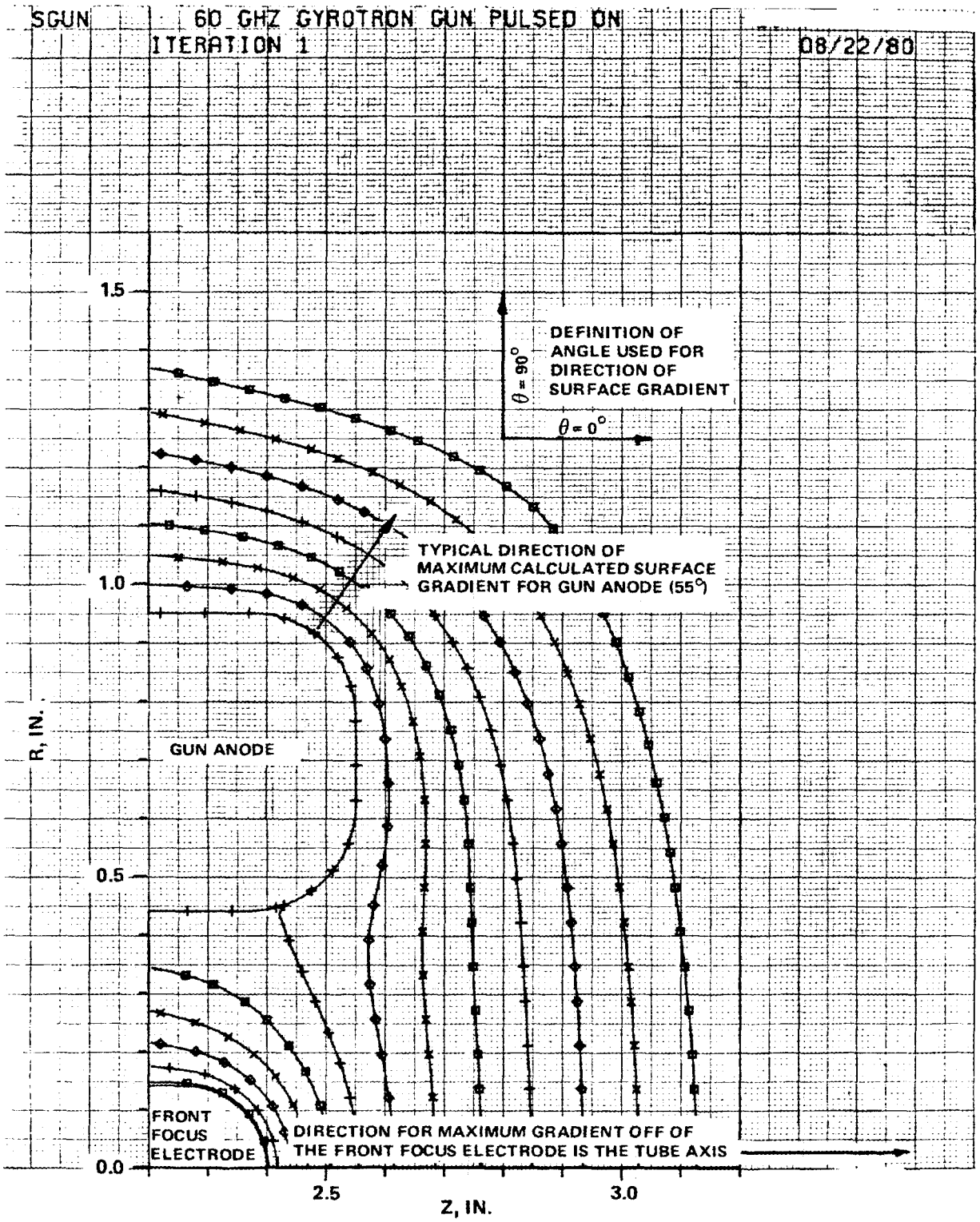

FIGURE 2: MAGNIFIED VIEW OF THE GRADIENTS FOR THE ORIGINAL GUN

A decision was made to attempt improvement of the gradient off of the gun anode. The most straightforward approach to this would be to increase the radius of curvature of the gun anode piece that had the maximum calculated surface gradient. If the maximum outside diameter and length of the gun anode were to remain constant (to preserve beam optics and ceramic gradients) a larger radius of curvature could easily be accommodated. This change in the shape of the gun anode is shown in the computer-generated plot of Figure 3, which shows the change in potential distribution when the new shape is used. The calculated maximum surface gradient was in the same direction as for the previous design, but the magnitude of the maximum gradient decreased by 20%. This relatively small change in gun design geometry accompanied by a very significant decrease in the maximum surface gradient should lessen the chances of arc formation in the gun.

For the case shown in Figure 3, the maximum voltage gradients at the gun anode and the tip of the cathode focus electrode are given in Table I for the on and off conditions.

TABLE I

Voltage Gradients

	ON	OFF
Gun Anode	60 kV/cm	90.5 kV/cm
Cathode Tip	119 kV/cm	42 kV/cm

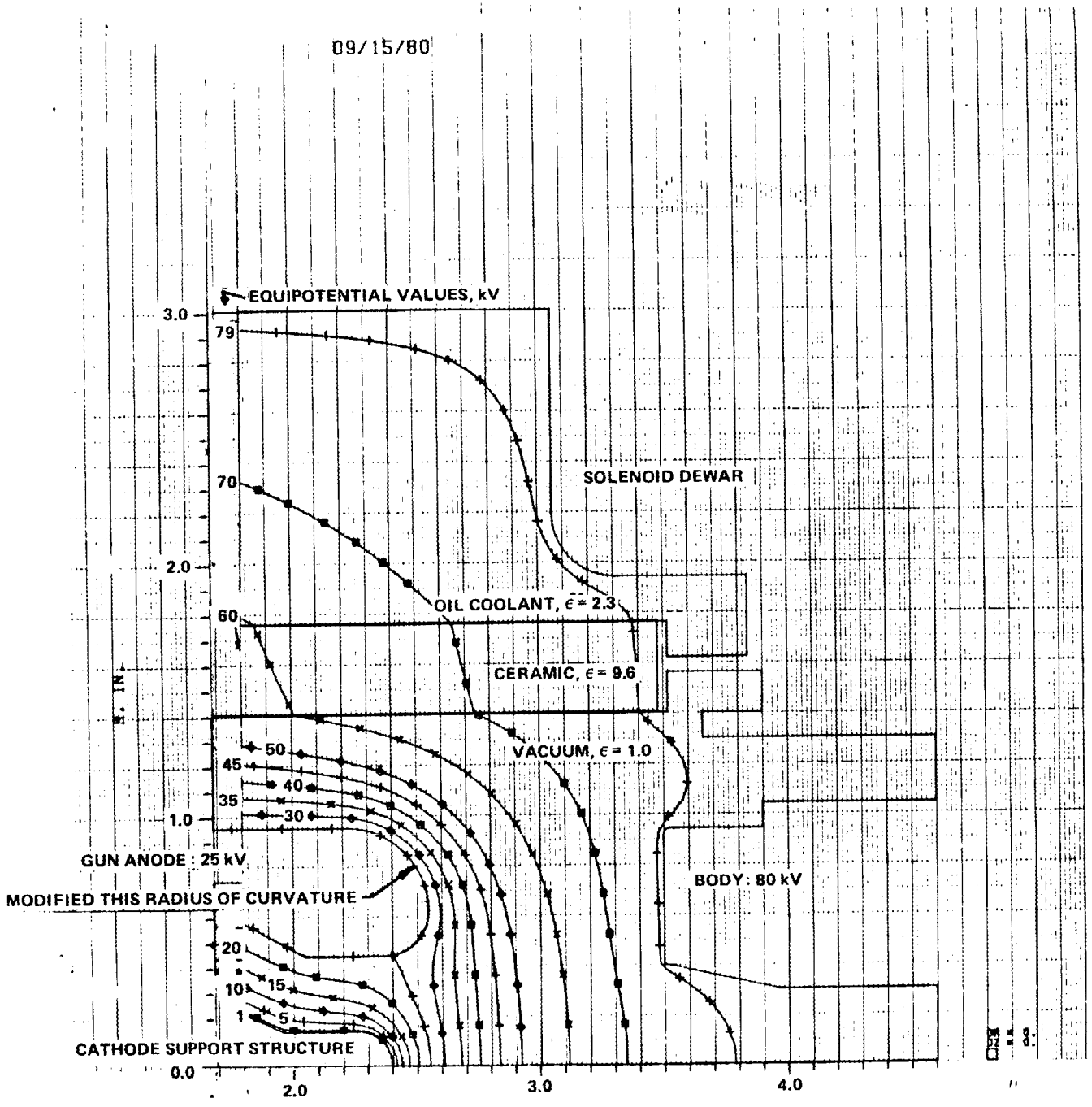

FIGURE 3: GRADIENTS FOR MODIFIED GUN

III. SUPERCONDUCTING SOLENOID MAGNET

The superconducting solenoid magnet is on order from Magnetic Corporation of America. Five milestones were established as follows:

1. Final design and review by Varian engineers
2. Receipt of conductor
3. Completion of magnet testing
4. Final testing of system
5. Delivery

The first two milestones are complete. The coils are being wound. The power supplies are complete and available for coil tests.

The gun coil and one half of the split pair have been wound. The remainder of the coils are now scheduled to be completed by October 3. Coil testing is now scheduled to be completed by October 10. The major dewar parts are complete with the exception of the top plate.

Final system tests are scheduled for the first week of November.

The pertinent cryogenic data for the superconducting solenoid magnet dewar are given in Table II.

TABLE II

Superconducting Solenoid Magnet Dewar Cryogenic Data

	Guaranteed	Calculated
Liquid Nitrogen Boiloff/Liters per Hour	0.17	0.13
Liquid Nitrogen Holdtime/Hours	120	160
Liquid Nitrogen/Total Volume in Liters	21	21
Liquid Helium Boiloff/Liters per Hour, Coil on*	0.70	0.56
Liquid Helium Boiloff/Liters per Hour, Coil on**	0.42	0.33
Liquid Helium Holdtime/Coil on*	32	41
Liquid Helium Holdtime/Coil off**	135	172
Liquid Helium Holdtime/Above the Coil Liters	23	23
Total Helium Volume/Liters	57	57

*Calculated with liquid helium above the coil only.
**Calculated with entire liquid helium volume.

IV. OUTPUT/COLLECTOR

A. MODE CONVERSION AT CONICAL-CYLINDRICAL TAPER JUNCTIONS

The work described in Section IV of Reference 9 has been extended to calculate mode power ratios, $P_{mn}(K)$, where the transductance parameter $K \equiv -\pi a\Theta_o/\lambda$, for values of $K \gtrsim 1$. Here, the parameter, a, is the cylindrical waveguide radius, Θ_o is the taper angle, and λ is the free space wavelength. For a cylindrical-conical junction the sign of K is reversed. However, as we will see below, the sign of K affects only the phase of the transduced modes and does not affect the amplitudes of the mode power ratios. The ratio of power converted into the TE_{om} mode from a pure incident TE_{on} mode was previously found to be

$$P_{mn}(K) = \frac{64\, X_{1m}^2\, X_{1n}^2}{(X_{1m}^2 - X_{1n}^2)^4} K^2, \text{ for } |K| < 1. \tag{1}$$

where X_{1n} is the nth positive root of $J_1(X) = 0$. In order to generalize (1) for $|K| > 1$ we use Equation (2) in Reference 9,

$$P_{mn}(K) = \frac{J_o^2\,(X_{1m})}{J_o^2\,(X_{1n})} \frac{|T_{mn}\,(K)|^2}{|T_{nn}\,(K)|^2}, \text{ for } |K| \lesssim 2.5, \tag{2}$$

where

$$T_{mn}(K) = \frac{2}{J_o^2\,(X_{1m})} \int_0^1 te^{ikt^2}\, J_1(X_{1m}t)\, J_1(X_{1n}t)dt \tag{3}$$

The integral in Equation (3) has been evaluated numerically for various (m, n) and K. The results are shown in Figures 4 - 9 where only the absolute values, $|T_{mn}(K)|$ vs $|K|$, as required by Equation (2) are given. The results agree with those quoted by Solymar[10] and those calculations have been extended to include m or n = 5, 6 and values of K in the range 2.5 - 10.

Using Equation (2) and the results for $|T_{mn}(K)|$, the mode conversion, $P_{mn}(K)$, has also been computed as shown in Figures 10 - 15. For values of

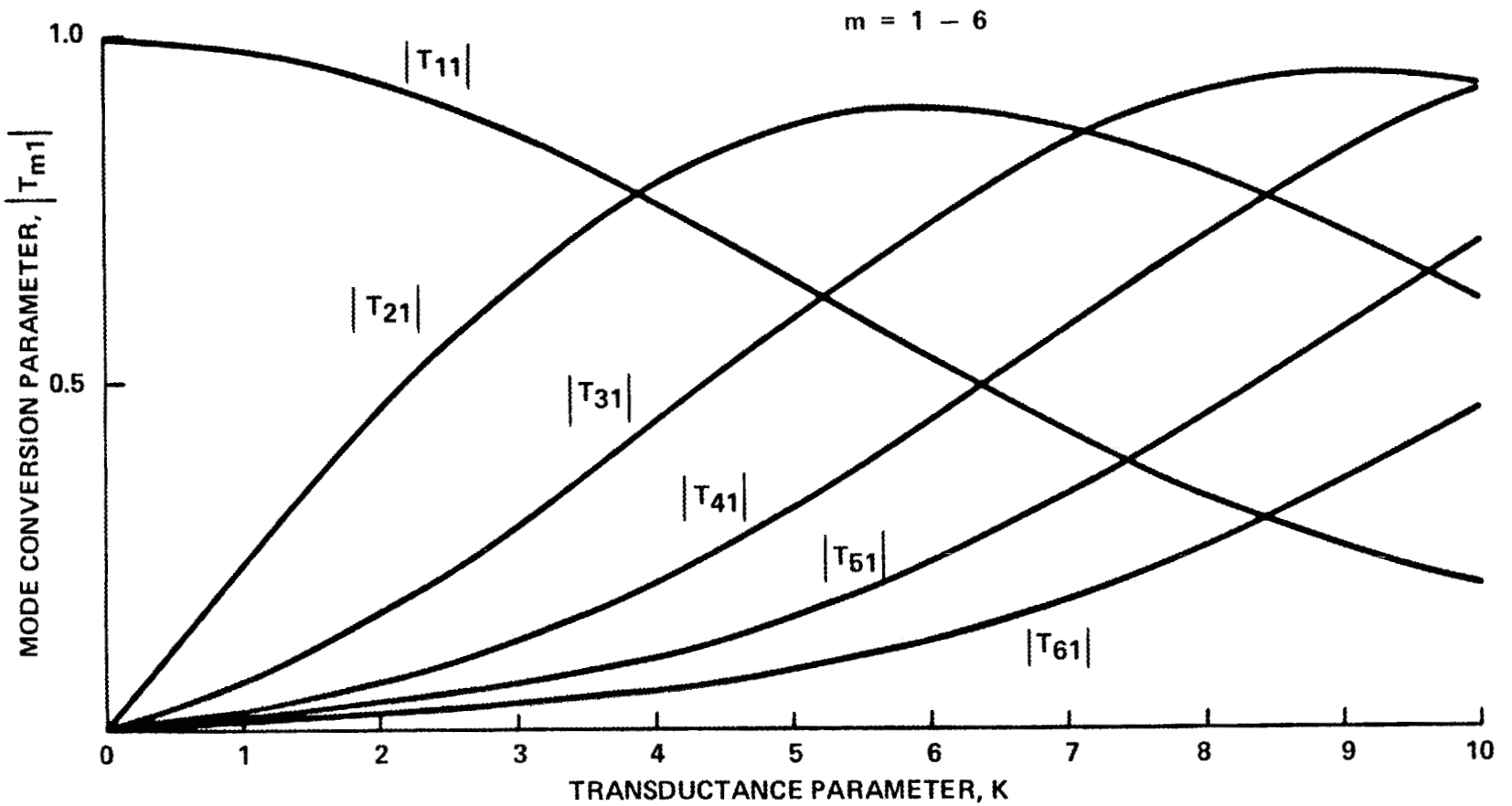

FIGURE 4: VARIATION OF THE MODE CONVERSION PARAMETER, $|T_{m1}|$, WITH THE TRANSDUCTANCE PARAMETER, K

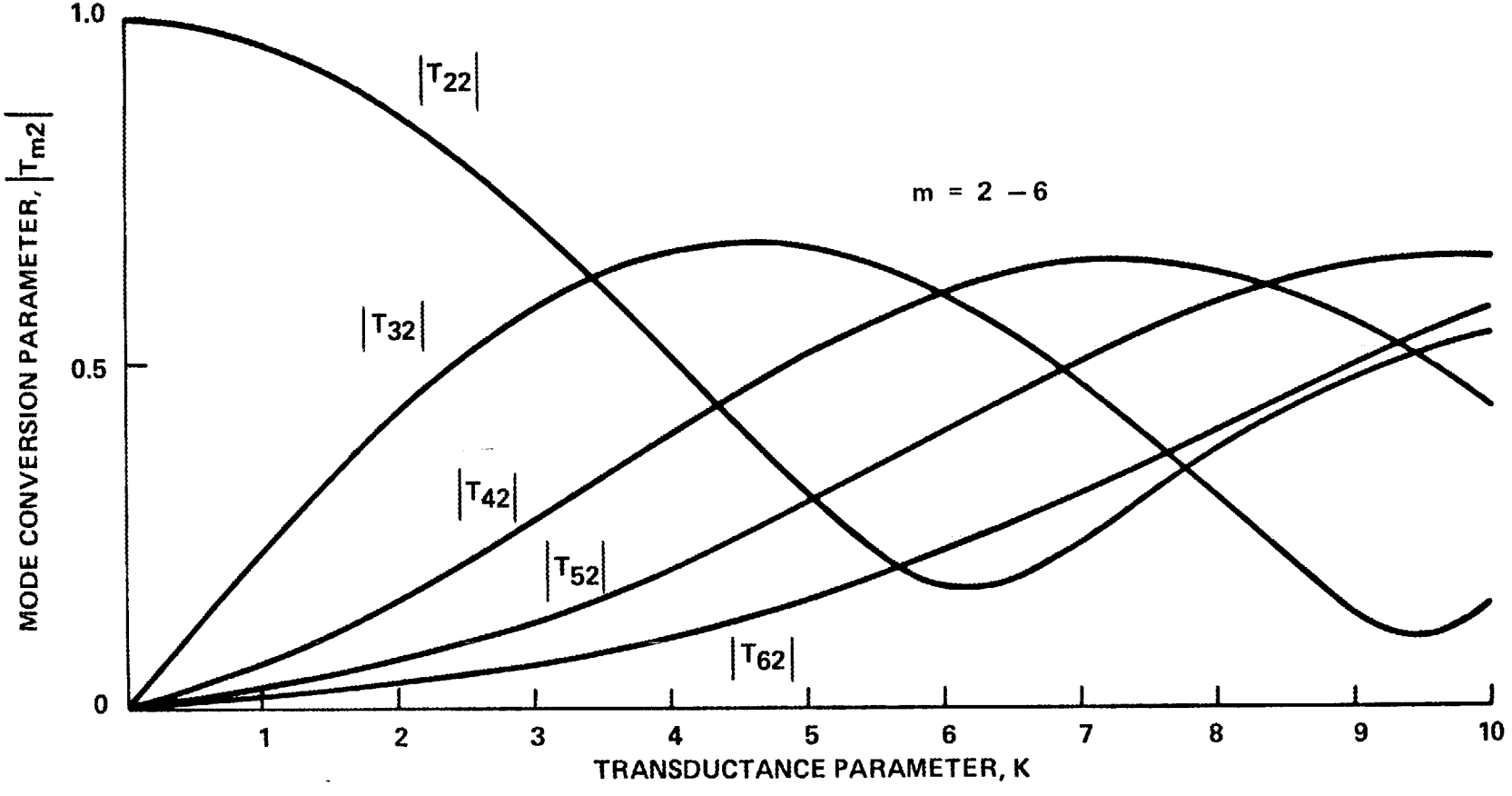

FIGURE 5: VARIATION OF THE MODE CONVERSION PARAMETER, $|T_{m2}|$, WITH THE TRANSDUCTANCE PARAMETER, K

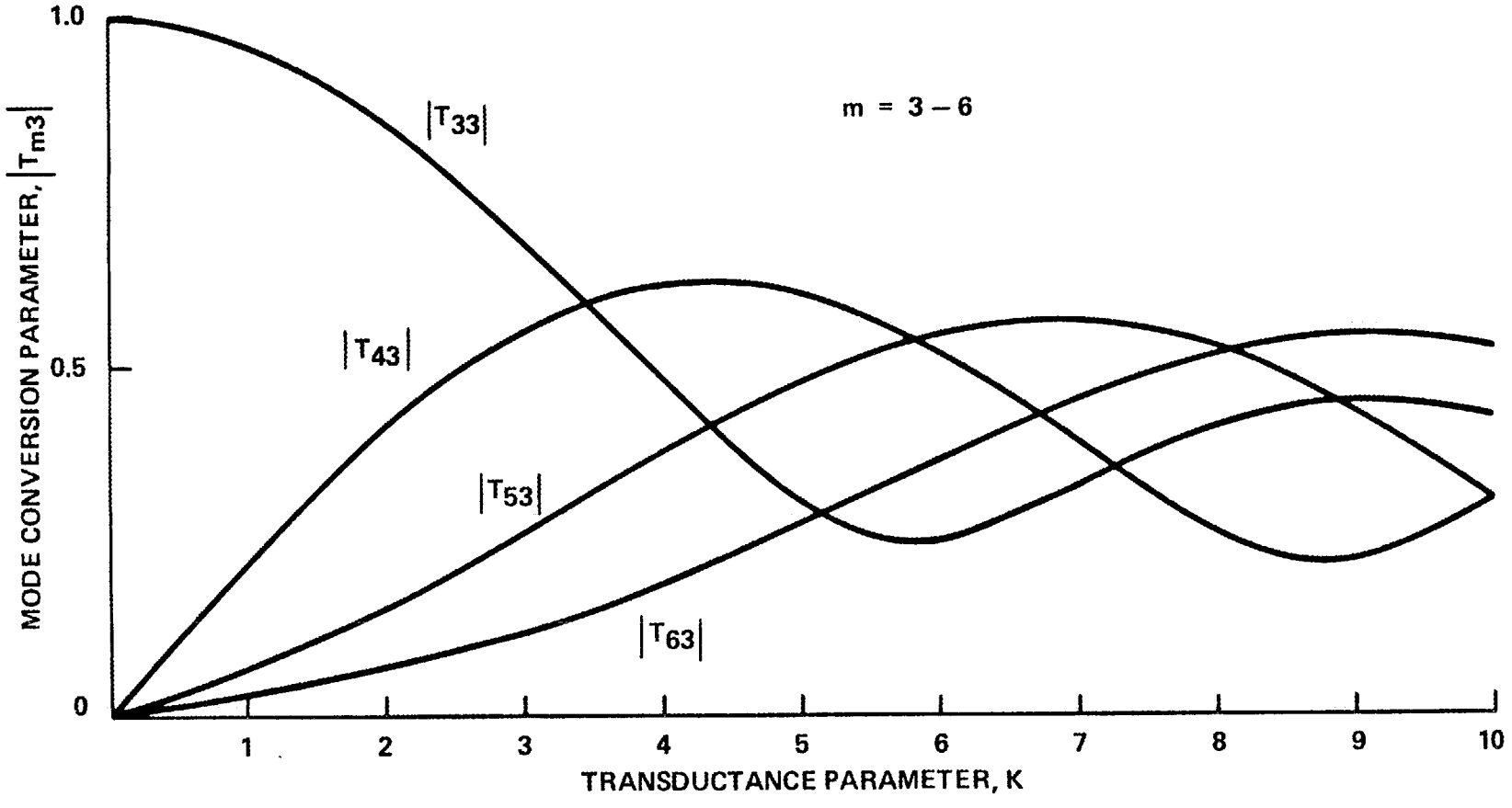

FIGURE 6: VARIATION OF THE MODE CONVERSION PARAMETER, $|T_{m3}|$, WITH THE TRANSDUCTANCE PARAMETER, K

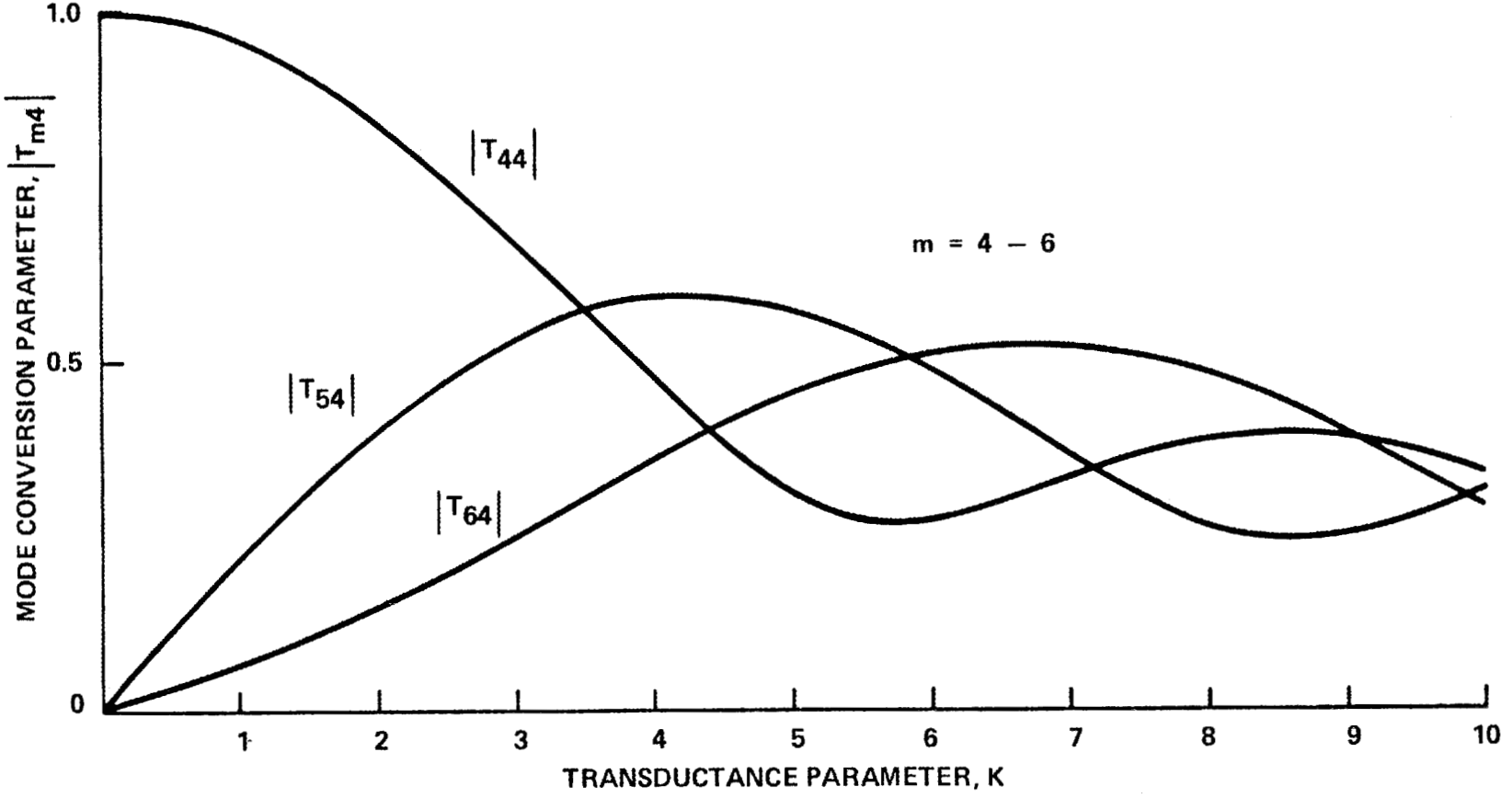

FIGURE 7: VARIATION OF THE MODE CONVERSION PARAMETER, $|T_{m4}|$, WITH THE TRANSDUCTANCE PARAMETER, K

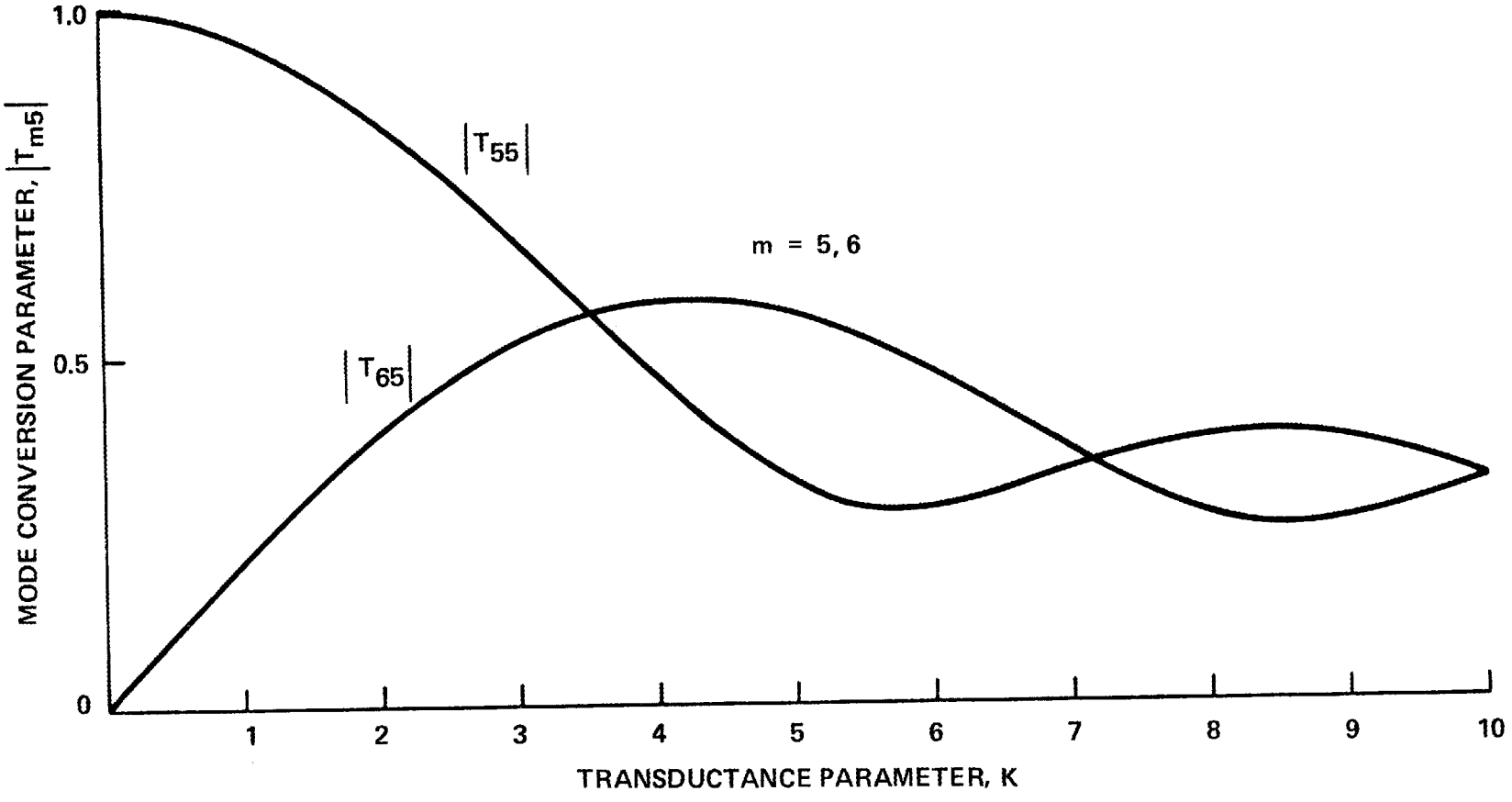

FIGURE 8: VARIATION OF THE MODE CONVERSION PARAMETER, $|T_{m5}|$, WITH THE TRANSDUCTANCE PARAMETER, K

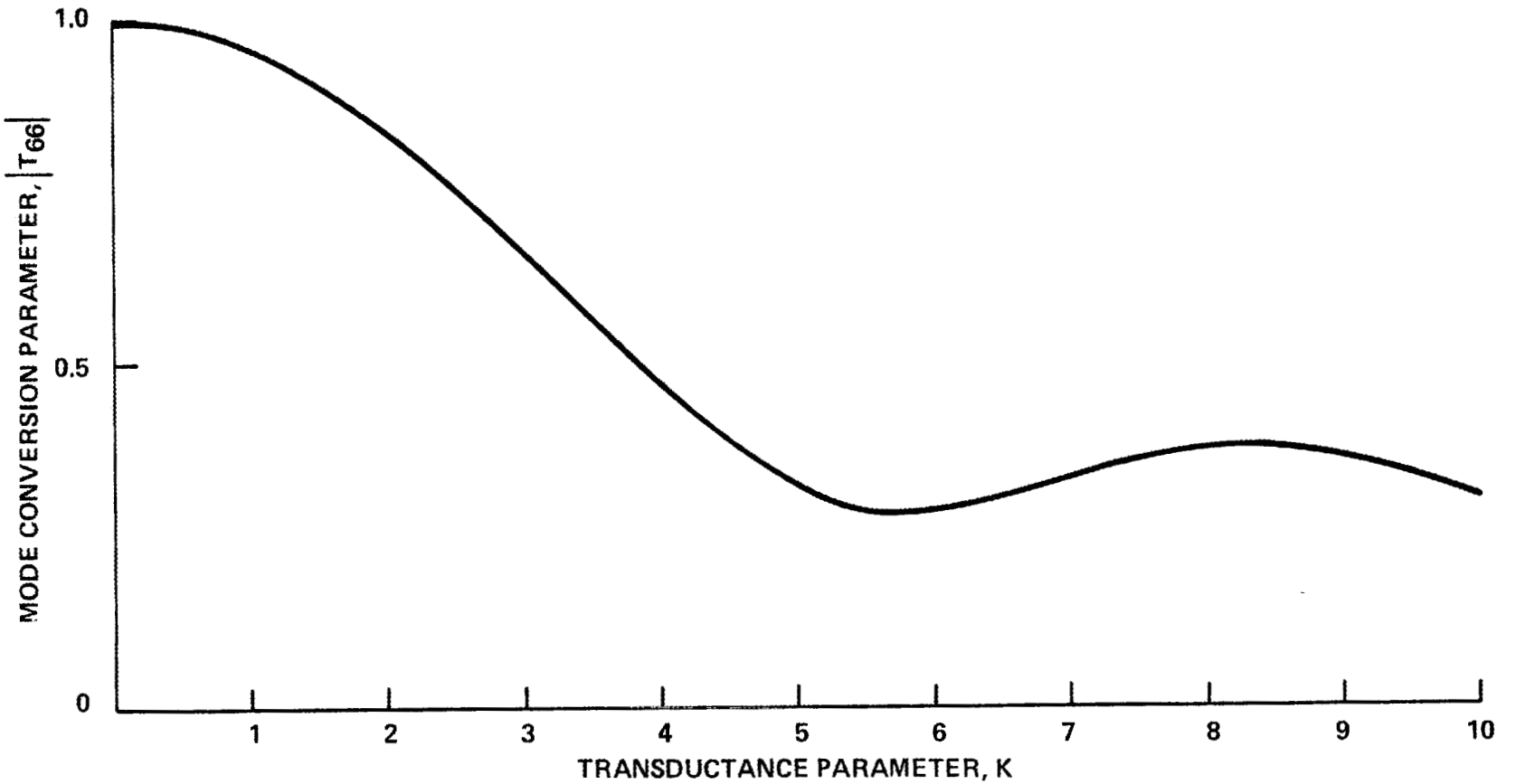

FIGURE 9: VARIATION OF THE MODE CONVERSION PARAMETER, $|T_{66}|$, WITH THE TRANSDUCTANCE PARAMETER, K

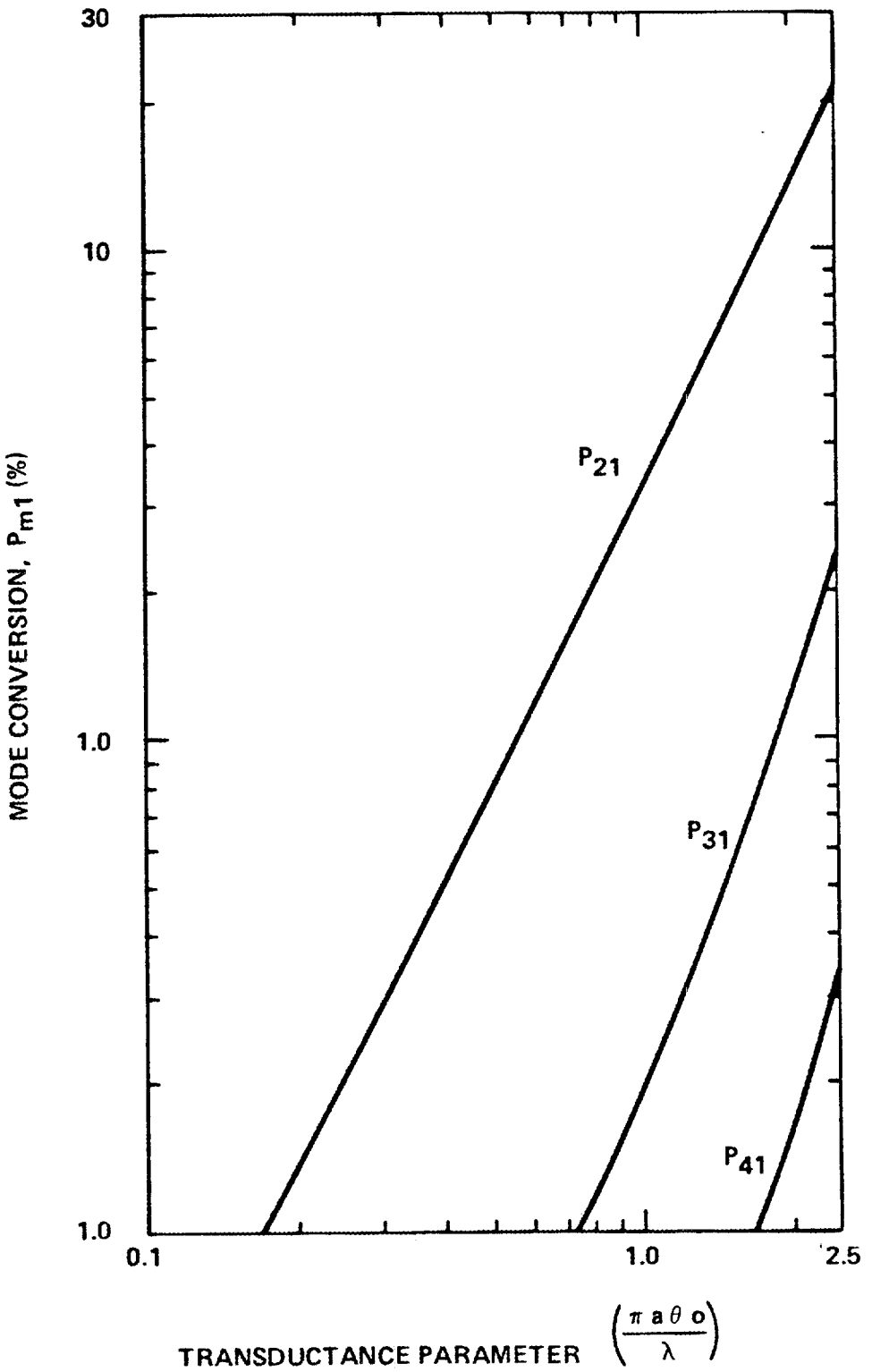

FIGURE 10: MODE CONVERSION, P_{m1}

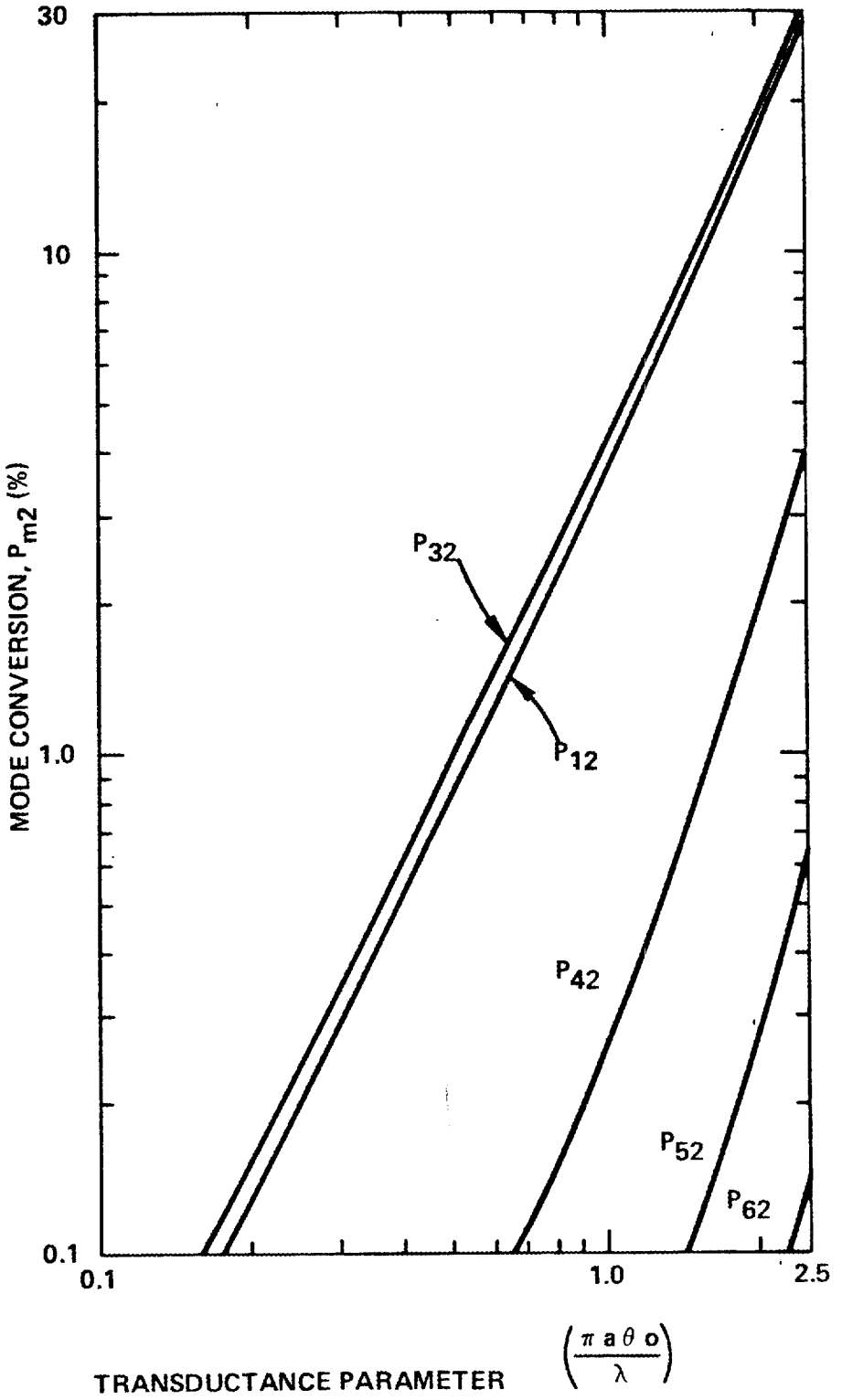

FIGURE 11: MODE CONVERSION, P_{m2}

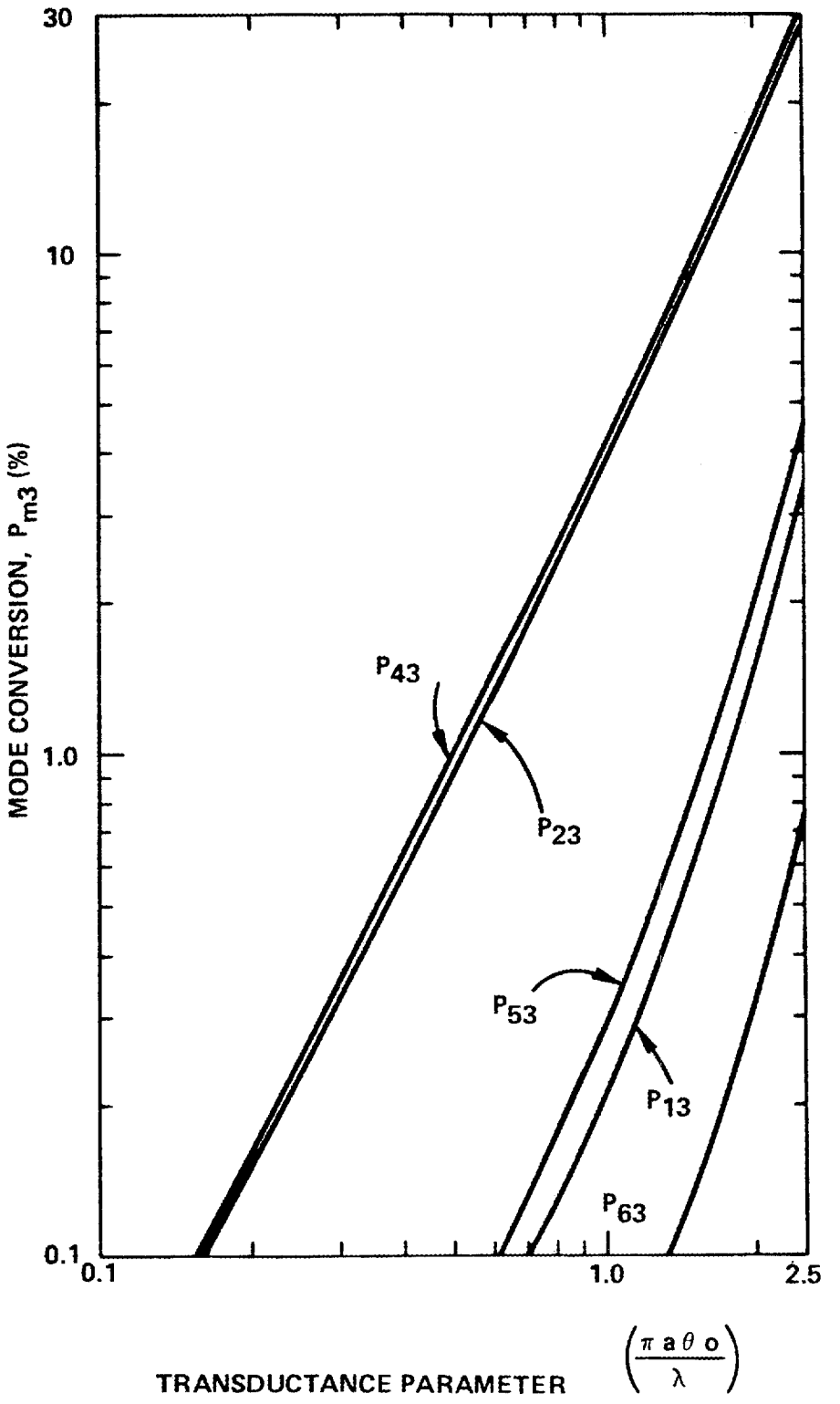

FIGURE 12: MODE CONVERSION, P_{m3}

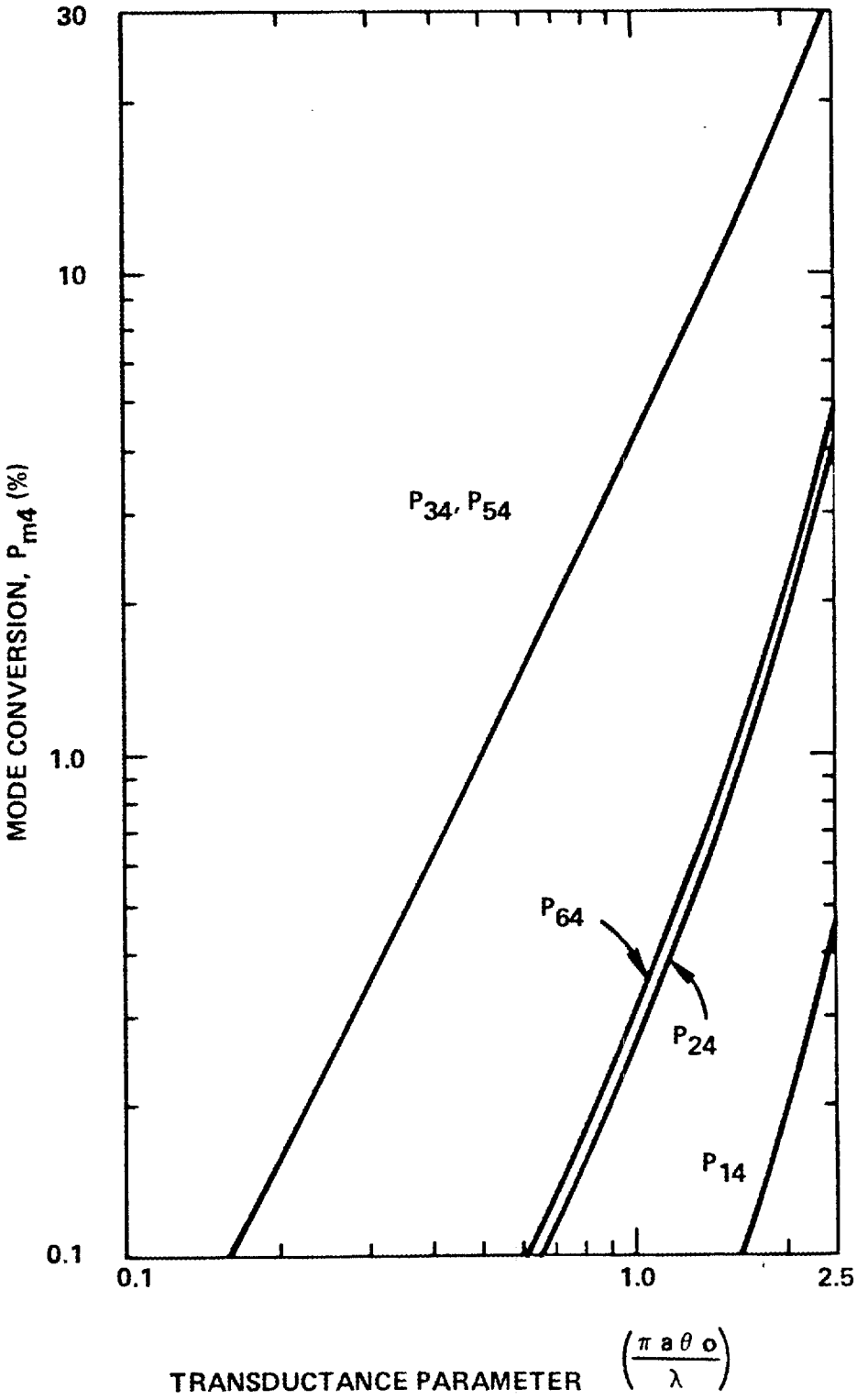

FIGURE 13: MODE CONVERSION, P_{m4}

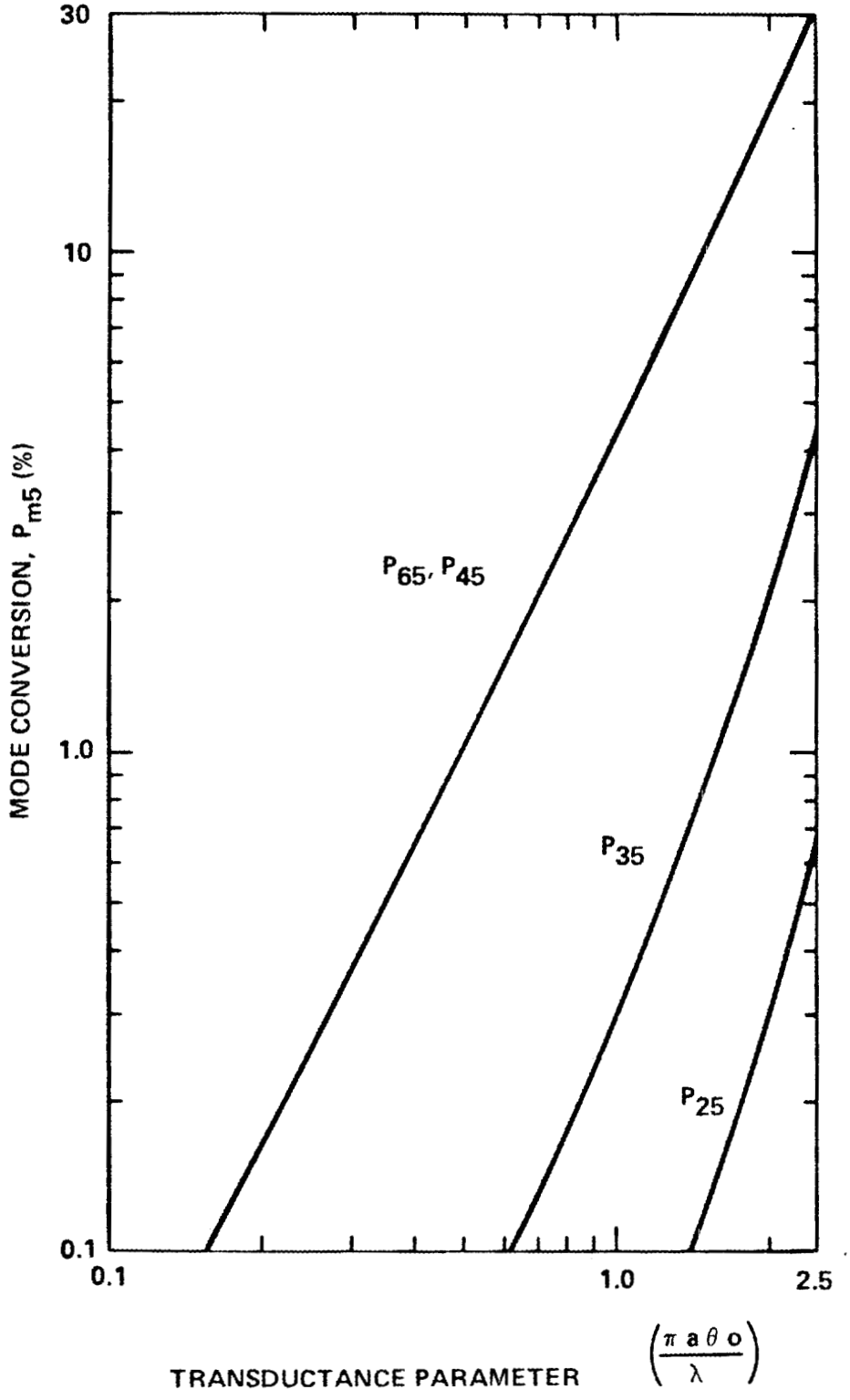

FIGURE 14: MODE CONVERSION, P_{m5}

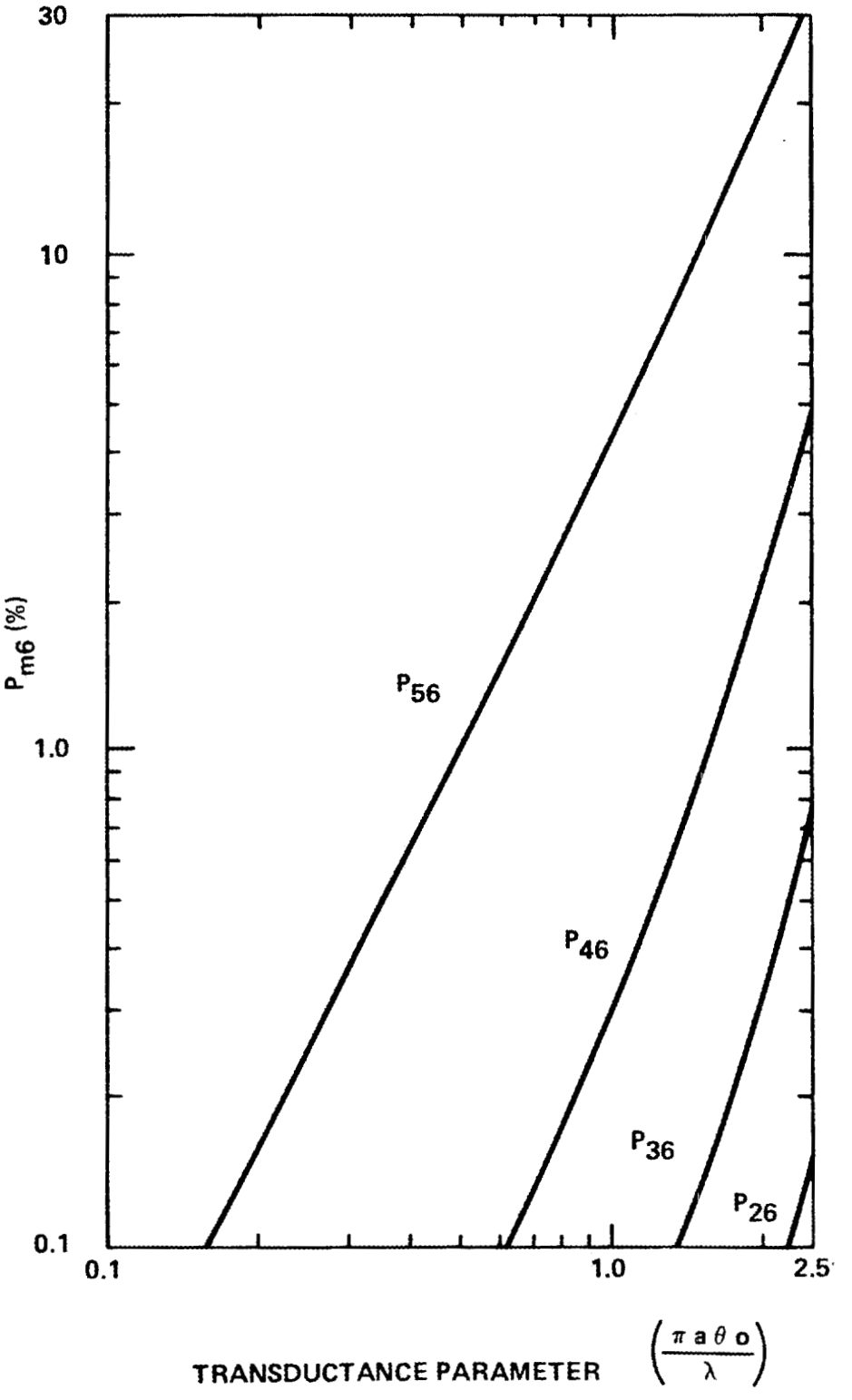

FIGURE 15: MODE CONVERSION, P_{m6}

$|K| \gtrsim 4$ these calculations yield physically meaningless results ($P_{mn} > 1$). Apparently, for $|K| \gtrsim 2.5$ the theoretical analysis of the problem is no longer correct. As the symptoms of this error in analysis are values of P_{mn} which exceed unity, one suspects that the boundary condition applied at the conical-cylindrical junction (see the Appendix in Reference 9) does not properly account for depletion of the pure incident TE_{on} wave during the mode conversion process. For this reason the region of validity of Equation (2) is limited to $|K| \lesssim 2.5$.

B. ELECTRON TRAJECTORY CALCULATIONS

A computer simulation of the electron beam was done for the CW tube collector design.

Twenty-four trajectories were calculated starting from the interaction circuit with eight electrons arranged about each of three orbit centers. Because of program size limitations, four axial collector segments were required in the calculation to reach the area where interception occurs.

The calculations were made using the fringing field of the superconducting magnet system with one additional coil in the collector region for field shaping.

It was necessary to use extremely high precision (35 digits) to calculate the off-axis vector potential from which the magnetic field is derived. The vector potential at each point was calculated by a Gaussian quadrature of the contributions from each coil. Each contribution was calculated by means of complete elliptic integrals obtained by the method of converging arithmetic-geometrical means. The extremely high precision was required in order to retain a few significant figures when two very nearly equal contributions of opposite sign are added.

Calculations of the trajectories in the region 20.5 to 67.5 inches from the center of the interaction circuit were made. The first trajectory intercepted approximately 20 inches beyond the lower collector seal. The

beam loading is spread over an axial length of approximately 2 feet. Table III shows the region of the collector impinged by each group of eight trajectories:

TABLE III

Collector Trajectory Landing Sites

Trajectory Group	Z (inches)
Outer	38.55 - 60.33
Middle	34.91 - 57.98
Inner	36.75 - 53.08

The tendency is for the outermost electrons at the beginning of this particular calculation to travel the furthest before impingement on the collector surface.

An estimate of the peak power density on the collector walls will require more detailed trajectory simulation runs.

V. WINDOW

The piece parts for the single disc BeO window have been received. The window braze fixture is due in mid-October at which time the assembly of the window for the experimental pulsed tube can be started.

VI. COMPONENTS

A variety of waveguide components is being developed for use with the 60 GHz gyrotron including waterloads, a frequency sampler and arc detector, and mode filters.

A. WATERLOADS

A modification to the flange design used on the 28 GHz waterload is being made to prevent flange arcing and heating anticipated at high CW powers in multimode waveguide systems. This flange design utilizes a disposable copper gasket captured by stainless steel flanges.

Both a pulsed and CW load are being designed. The pulsed waterload design allows more turbulent flow at lower water flow rates and has a smaller thermal mass.

Construction of the first pulsed waterload is scheduled to start in October.

B. FREQUENCY SAMPLER AND ARC DETECTOR

A combination frequency sampler and arc detector has been designed. The frequency sampler portion is designed to monitor all TE modes. The light sensing portion is designed to cut off up to the third harmonic of the design operating frequency of the gyrotron to prevent rf leakage into the fiber optics light guides. An improvement in the test lamp portion of the arc detector is being made to ensure a more reliable test function.

Check prints of the frequency sampler and arc detector are completed and are being reviewed for engineering approval.

C. MODE FILTERS

Two types of mode filters are being designed. The first type is a water-cooled stainless steel waveguide, which utilizes the differential in

loss between non-circular electric modes and circular electric modes for filtering. Check prints for this first type of mode filter have just been completed. The second type of mode filter consists of alternating stainless steel rings and gaps backed up by a waterloaded ceramic cylinder. In addition to the mode filtering mechanism of the first type of mode filter the second type creates breaks in the conducting wall for non-circular electric modes but not for circular electric modes. Some of the cold test parts have been received for this design.

VII. TUBE ASSEMBLY

A. VGE-8060 S/N X-1 (FIRST EXPERIMENTAL PULSED TUBE)

Essentially all of the piece parts for S/N X-1 have been received and construction is well under way. Construction is expected to be completed by the end of October.

The collector assembly is ready for its final braze.

The collector extension assembly, the 2.5 inches inside diameter waveguide between the collector and window, is in process.

A braze fixture is being made for the collector ceramic assemblies.

A braze fixture for the single disc beryllia window will be complete in mid-October.

The output taper assembly, the taper loading from the output cavity to the collector has been brazed. A fixture is being made to accomplish the final machine operation.

A braze fixture for the final brazes of the beam shaver and output assembly, the assembly consisting of the anode and output cavity, is being made.

The final cathode assembly is under construction and is expected to be completed by October 10.

B. VGE-8060 S/N 1 (FIRST 100 ms PULSE DURATION TUBE)

Ninety percent of the piece parts for the first 100 ms pulse duration gyrotron have been received. Construction has started and is expected to be completed by the end of December.

The collector assembly is ready for its final braze.

The output taper assembly has been brazed.

C. VGE-8060 S/N 2 (SECOND 100 ms PULSE DURATION TUBE)

Ninety percent of the piece parts for the second 100 ms pulse duration gyrotron have been received. Construction is scheduled to begin in November.

VIII. PROGRAM SCHEDULE AND PLANS

The milestone chart and status report is shown in Figure 16.

For the first experimental pulsed gyrotron, model number VGE-8060 serial number X-1, all gun parts have been received, assembly has started and the first gun is expected by October 10.

The superconducting solenoid magnet is being wound at Magnetic Corporation of America following a successful design review in July. Delivery is expected as early as mid-November.

Piece parts for the interaction circuit portion of the tube have been received. Assembly has started. A braze jig is being made for the final assembly brazes.

Piece parts for the window are available. A braze jig is being made for the window braze.

Assembly of the first experimental pulsed gyrotron is scheduled for completion by the end of October.

Ninety percent of the piece parts for the first 100 ms pulse duration gyrotron have been received. Assembly has started and is scheduled to be completed by the end of December.

Building of the pulsed waterload and frequency sampler and arc detector will start in October.

Ninety percent of the piece parts for the second 100 ms pulse duration gyrotron have been received. Assembly is planned to start in November.

Modification of the Nike Zeus test set, funded by a separate contract is planned to be completed, at least for short pulse capability, by the first of January. At present, test set modification appears to be the limiting item.

MILESTONE CHART AND STATUS REPORT

○ ORIGINAL START □ REVISED START △ MAJOR MILESTONE
▽ INTERMEDIATE OR DECISION POINT ◇ PROPOSED SCHEDULED DEVIATION FOR A MAJOR MILESTONE
STATUS REPORT TIME — ACTIVITY SCHEDULED ▬ ACTIVITY COMPLETED

PROGRAM: 60 GHz DEVELOPMENT

JOB NO.:

STATUS REPORT DATE: SEPTEMBER 1980

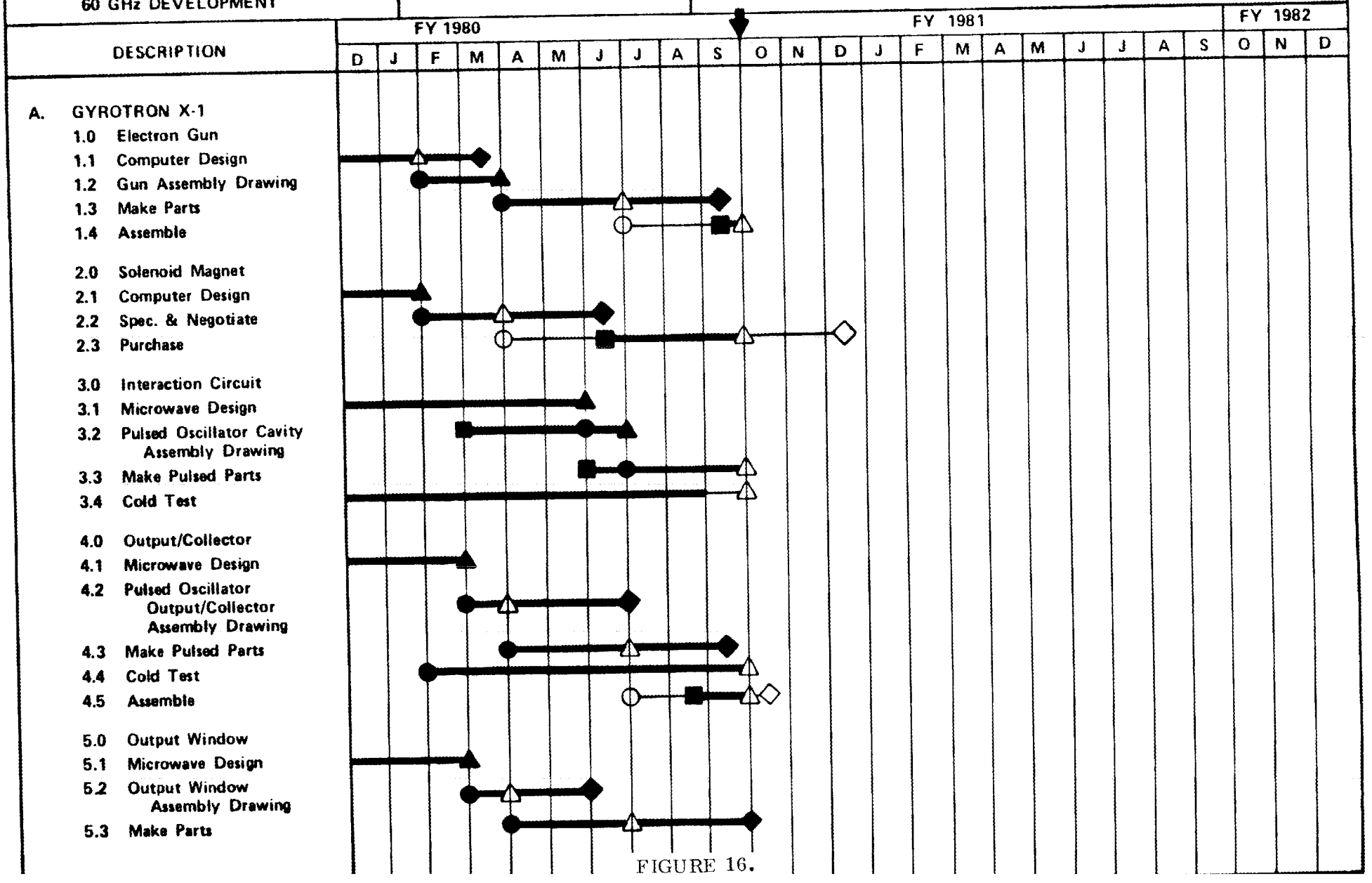

FIGURE 16.

MILESTONE CHART AND STATUS REPORT

○ ORIGINAL START · □ REVISED START · △ MAJOR MILESTONE
▽ INTERMEDIATE OR DECISION POINT · ◇ PROPOSED SCHEDULED DEVIATION FOR A MAJOR MILESTONE
↓ STATUS REPORT TIME · —— ACTIVITY SCHEDULED · ▬ ACTIVITY COMPLETED

PROGRAM: 60 GHz DEVELOPMENT

JOB NO.:

STATUS REPORT DATE: SEPTEMBER 1980

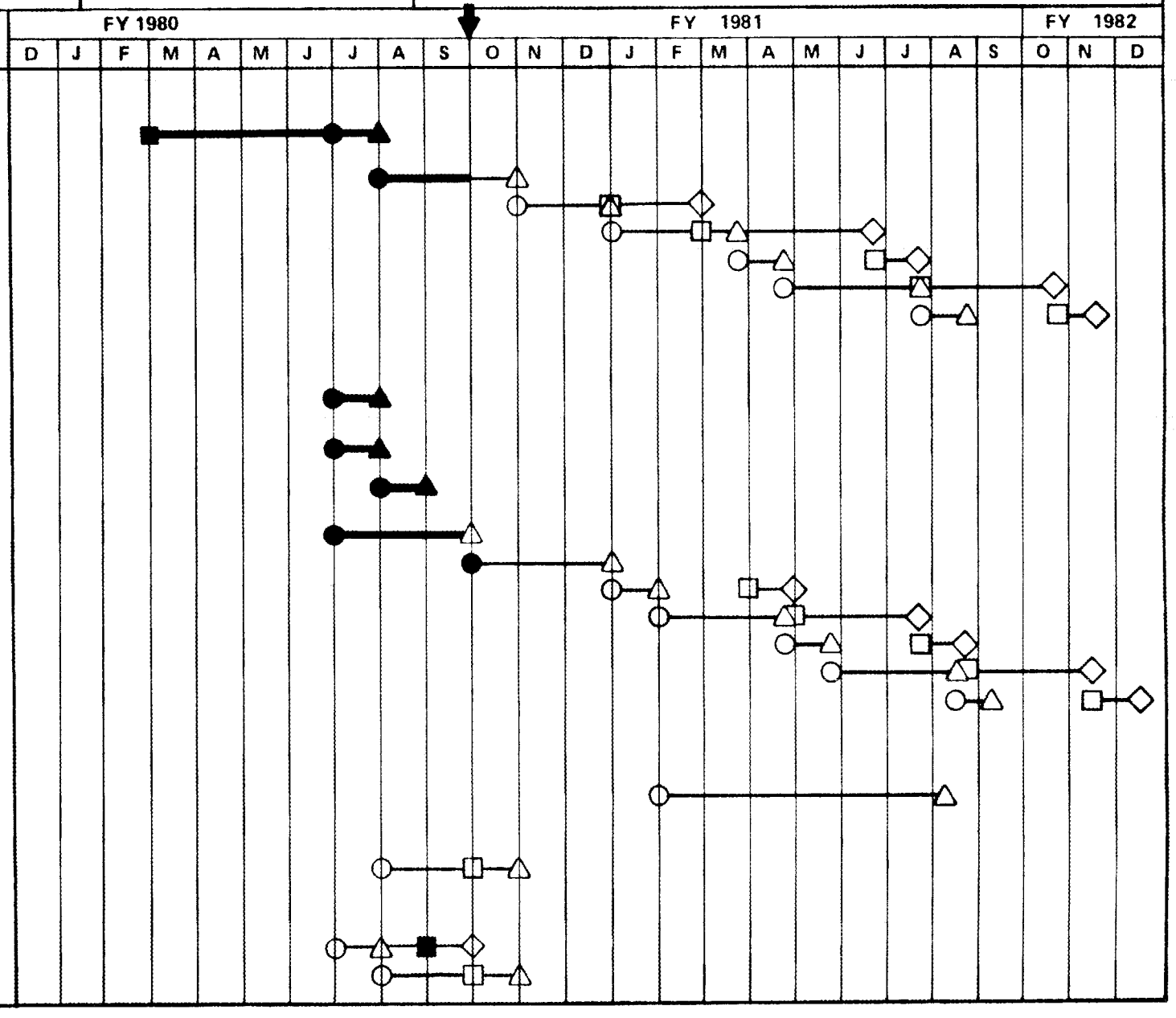

MILESTONE CHART AND STATUS REPORT

○ ORIGINAL START □ REVISED START △ MAJOR MILESTONE
▽ INTERMEDIATE OR DECISION POINT ◇ PROPOSED SCHEDULED DEVIATION FOR A MAJOR MILESTONE
STATUS REPORT TIME — ACTIVITY SCHEDULED ▬ ACTIVITY COMPLETED

PROGRAM: 60 GHz DEVELOPMENT

JOB NO.:

STATUS REPORT DATE: SEPTEMBER 1980

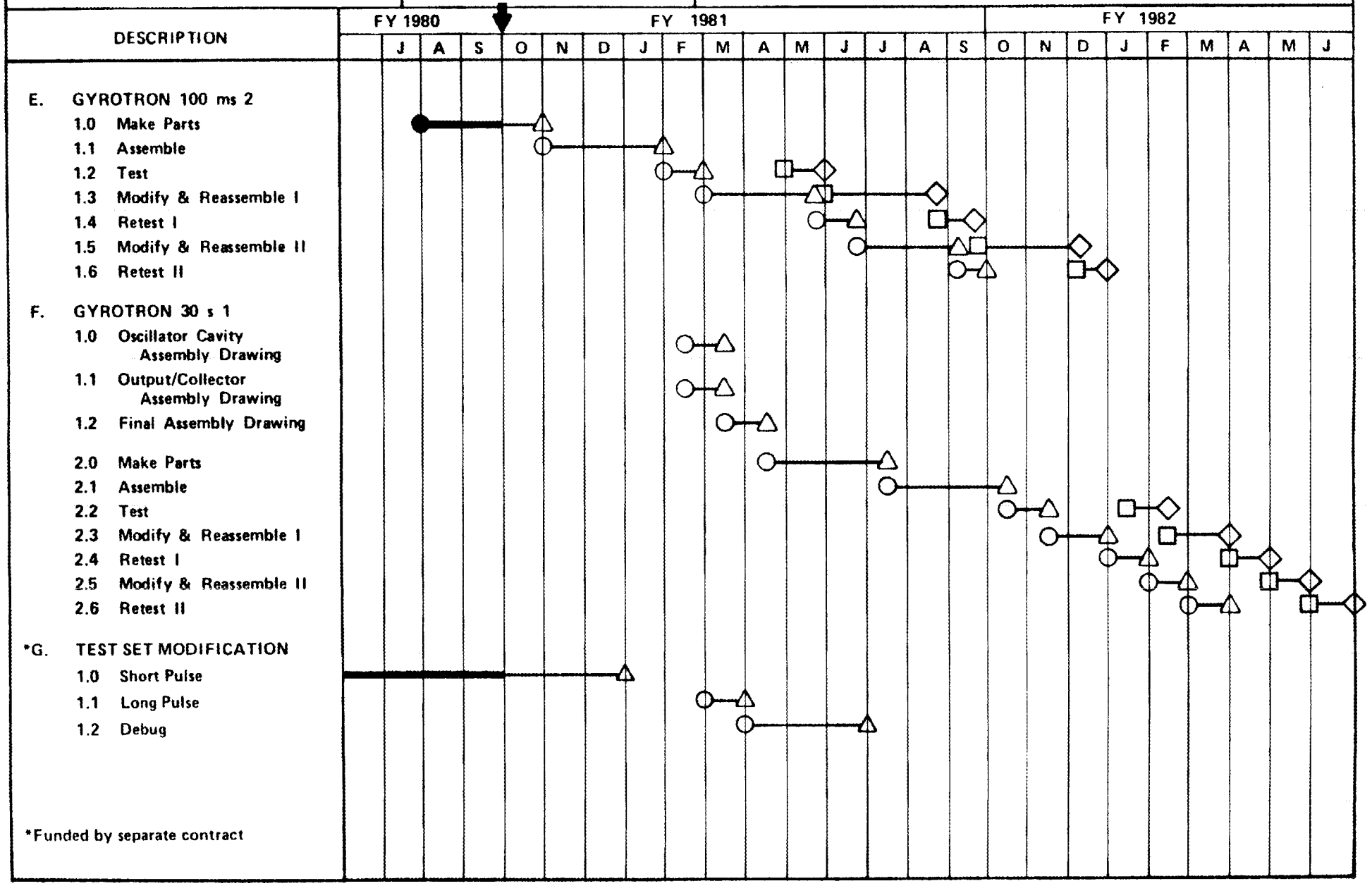

*Funded by separate contract

MILESTONE CHART AND STATUS REPORT

○ ORIGINAL START
□ REVISED START
△ MAJOR MILESTONE
▽ INTERMEDIATE OR DECISION POINT
◇ PROPOSED SCHEDULED DEVIATION FOR A MAJOR MILESTONE
STATUS REPORT TIME
— ACTIVITY SCHEDULED
▬ ACTIVITY COMPLETED

PROGRAM: 60 GHz DEVELOPMENT

JOB NO.:

STATUS REPORT DATE: SEPTEMBER 1980

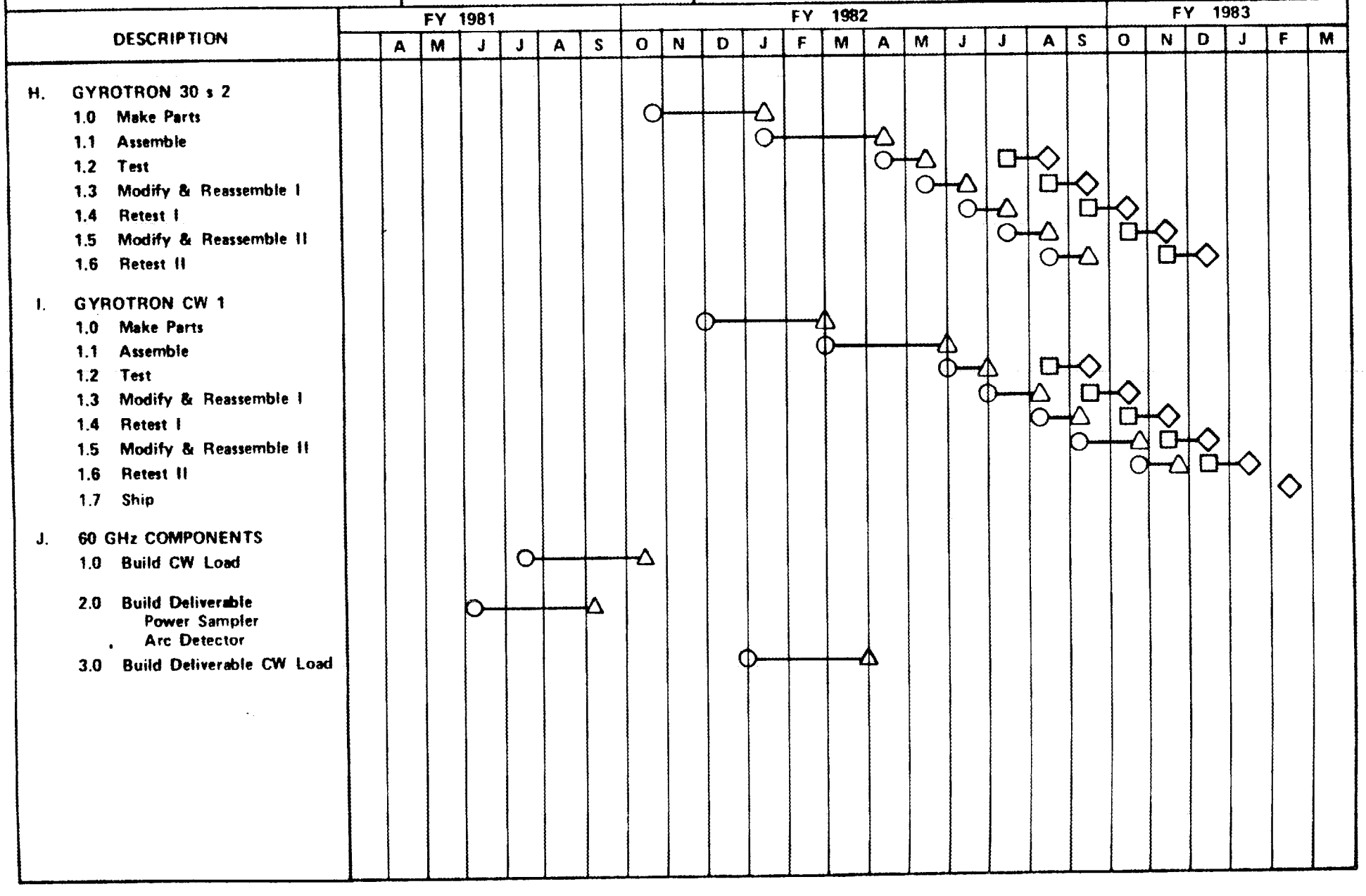

MILESTONE CHART AND STATUS REPORT

○ ORIGINAL START □ REVISED START △ MAJOR MILESTONE
▽ INTERMEDIATE OR DECISION POINT ◇ PROPOSED SCHEDULED DEVIATION FOR A MAJOR MILESTONE
STATUS REPORT TIME — ACTIVITY SCHEDULED ▬ ACTIVITY COMPLETED

PROGRAM: 60 GHz DEVELOPMENT

JOB NO.

STATUS REPORT DATE: SEPTEMBER 1980

DESCRIPTION	FY 1982										FY 1983												FY 1984		
	D	J	F	M	A	M	J	J	A	S	O	N	D	J	F	M	A	M	J	J	A	S	O	N	D
K. GYROTRON CW 2																									
1.0 Make Parts																									
1.1 Assemble																									
1.2 Test																									
1.3 Modify & Reassemble I																									
1.4 Retest I																									
1.5 Modify & Reassemble II																									
1.6 Retest II																									
1.7 Ship																									
L. WINDOW 1																									
1.0 Make Parts																									
1.1 Assemble																									
M. WINDOW 2																									
1.0 Make Parts																									
1.1 Assemble																									
N. WINDOW 3																									
1.0 Make Parts																									
1.1 Assemble																									

IX. REFERENCES

1. H. R. Jory, E. L. Lien, and R. S. Symons, Final Report, "Millimeter Wave Study Program", Oak Ridge National Laboratory Order No. Y12 11Y-49438 V, Varian Associates, Inc., November 1975.

2. D. V. Kisel, G. S. Korablev, V. G. Navel'yev, M. I. Petelin and Sh. E. Tsimring, "An Experimental Study of a Gyrotron, Operating at the Second Harmonic of the Cyclotron Frequency, with Optimized Distribution of the High Frequency Field," Radio Engineering and Electronic Physics, Vol. 19, No. 4, 95-100, 1974.

3. S. Hegji, H. Jory and J. Shively, "Development Program for a 200 kW CW, 28 GHz Gyroklystron" Quarterly Report No. 6, Union Carbide Corporation Contract No. 53X01617C, Varian Associates, Inc., July through September 1977.

4. H. Jory, S. Evans, S. Hegji, J. Shively, R. Symons and N. Taylor "Development Program for a 200 kW, CW, 28 GHz Gyroklystron", Quarterly Report No. 9, Union Carbide Corporation Contract No. W-7405-eng-26, ORNL Sub-01617/9, Varian Associates, Inc., April through June 1978.

5. V. A. Flyagin, et al, "The Gyrotron", IEEE Trans. MTT-25, No. 6 pp. 522-527, June 1977.

6. J. F. Shively et al, "Recent Advances in Gyrotrons," 1980 IEEE MTT-S International Microwave Symposium Digest, 28-30 May 1980, Washington, D.C. IEEE Catalog No. 80CH1545-3 MTT, pp 99-101.

7. F. Friedlander, E. Galli, H. Jory, F. Kinney, K. Miller, J. Shively and R. Symons, "Development Program for a 200 kW, CW, 28 GHz Gyroklystron", Quarterly Report No. 1, Union Carbide Corporation Contract No. 53X01617C, Varian Associates, Inc., October 1976.

8. F. Friedlander, E. Galli, H. Jory, K. Miller, J. Shively, and R. Symons, "Development Program for a 200 kW, CW, 28 GHz Gyroklystron," Quarterly Report No. 2, Union Carbide Corporation Contract No. 53X01617C, Varian Associates, Inc. October 1976.

9. J. F. Shively, D. S. Stone, and G. E. Wendell, "60 GHz Gyrotron Development Program", Quarterly Report No. 3, January through March 1980, Union Carbide Contract 53Y-21453C, Varian Associates, Inc.

10. L. Solymar, "Monotonic Multi-Section Tapers for Overmoded Circular Waveguide," IRE-MTT, 1959, p. 121.

ORNL/Sub-79/21453/5
October 6, 1980

INTERNAL DISTRIBUTION

1. L. A. Berry
2. A. L. Boch
3. J. L. Burke
4. R. J. Colchin
5-8. H. O. Eason
9. O. C. Eldridge
10. R. P. Jernigan
11-13. C. M. Loring
14. H. C. McCurdy
15. O. B. Morgan, Jr.
16. G. F. Pierce
17. T. L. White
18-19. Laboratory Records Department
20. Laboratory Records, ORNL-RC
21. Y-12 Document Reference Section
22-23. Central Research Library
24. Fusion Energy Division Library
25. Fusion Energy Division Communications Center
26. ORNL Patent Office

EXTERNAL DISTRIBUTION

27. R. A. Dandl, 1122 Calle De Los Serranos, San Marcos, CA 92069
28. R. J. DeBellis, McDonnell Douglas Astronautics Co., P.O. Box 516, St. Louis, MO 63166
29. A. N. Dellis, Culham Laboratory, Abingdon, Oxon, England, OX143DB
30. W. P. Ernst, Princeton University, Plasma Physics Laboratory, P.O. Box 451, Princeton, NJ 08540
31. W. Friz, AFAL/DHM, Wright Patterson AFB, OH 45433
32. T. Godlove, Particle Beam Program, Office of Inertial Fusion, Department of Energy, Mail Stop C-404, Washington, DC 20545
33. V. L. Granatstein, Naval Research Laboratory, Code 6740, Washington, DC 20375
34. G. M. Haas, Component Development Branch, Office of Fusion Energy (ETM), Department of Energy, Mail Stop G-234, Washington, DC 20545
35. J. L. Hirshfield, Yale University, Department of Engineering and Applied Science, P.O. Box 2159, Yale Station, New Haven, CT 06520
36. H. Ikegami, Institute of Plasma Physics, Nagoya University, Nagoya 464, Japan
37. J. V. Lebacqz, Stanford Linear Accelerator Center, P.O. Box 4349, Stanford, CA 94305
38. W. Lindquist, Electronics Engineering Department, Lawrence Livermore Laboratory, P.O. Box 808/L-443, Livermore, CA 94550
39. K. G. Moses, TRW Defense & Space Systems, 1 Space Park, Bldg. R-1, Redondo Beach, CA 90278
40. M. R. Murphy, Office of Fusion Energy (ETM), Department of Energy, Mail Stop G-234, Washington, DC 20545
41. V. B. Napper, Three Dunwoody Park, Suite 112, Atlanta, GA 30341
42. B. H. Quon, TRW Defense & Space Systems, 1 Space Park, Bldg. R-1, Redondo Beach, CA 90278
43. M. E. Read, Naval Research Laboratory, Code 6740, Washington, DC 20375
44. D. B. Remsen, General Atomic Company, P.O. Box 81608, San Diego, CA 92138
45. B. Stallard, Lawrence Livermore Laboratory, University of California, L-437, P.O. Box 808, Livermore, CA 94550
46. H. S. Staten, Office of Fusion Energy (ETM), Department of Energy, Mail Stop G-234, Washington, DC 20545
47. P. Tallerico, AT-1, Accelerator Technology Division, Los Alamos Scientific Laboratory, Mail Stop 817, P.O. Box 1663, Los Alamos, NM 87545

48. J. J. Tancredi, Hughes Aircraft Company, Electron Dynamics Division, 3100 W. Lomita Blvd., Torrance, CA 90509
49. R. J. Temkin, National Magnet Laboratory, Massachusetts Institute of Technology, Cambridge, MA 02139
50. A. Trivelpiece, Science Applications, Inc., 1200 Prospect Street, P.O. Box 2351, LaJolla, CA 92038
51. Director, U.S. Army Ballistic Missle Defense Advance Technology Center, Attn.: D. Schenk, ATC-R, P.O. Box 1500, Huntsville, AL 35807

52-53. Department of Energy Technical Information Center, Oak Ridge, TN 37830

54. RADC/OCTP, Griffiss AFB, NY 13441
55. Office of Assistant Manager for Energy Research and Development, Oak Ridge Operations Office, Department of Energy, Oak Ridge, TN 37830

UCN-13164
(3 6-78)
AUTHOR INDEX
11 5/16 x 14 11/16 PHOTOMASTER (DOUBLE 4 1/16 x 11 5/8 COLUMN)
75.0% REDUCTION (FINISH SIZE 8 1/2 x 11 - DOUBLE 3 1/16 x 8 11/16 COLUMN)

VARIAN DISTRIBUTION

56.	R. Berry
57.	S. Evans
58.	P. Ferguson
59.	T.J. Grant
60.	G. Jacobson
61.	H. Jory
62.	A.L. Nordquist
63.	J. Moran
64-69.	J.F. Shively
70.	A. Staprans
71.	D. Stone
72.	R. Symons
73-75.	R.M. West